

## ADAPTIVE VARIABLE IMPEDANCE APPLIED TO ROBOTIC REHABILITATION OF WALKING

Guido G. Penã<sup>1</sup>, Samuel L. Nogueira<sup>2</sup>, Leonardo J. Consoni<sup>1</sup>, Wilian M. dos Santos<sup>1</sup>, Juan Carlos Perez-Ibarra<sup>1</sup>, Adriano A. G. Siqueira<sup>1</sup>

<sup>1</sup> University of São Paulo (USP), Engineering School of São Carlos, Mechanical Engineering Department; Center for Advanced Studies in Rehabilitation (NEAR-USP); and Center for Robotics of São Carlos (CROB-USP), São Carlos, Brazil, [siqueira@sc.usp.br](mailto:siqueira@sc.usp.br)

<sup>2</sup> Federal University of São Carlos (UFSCar), São Carlos, Brazil

**Abstract:** This paper describes the preliminary results of an adaptive variable impedance strategy designed for robot-aided walking rehabilitation of post-stroke patients. The proposed adaptive strategy considers the control of the mechanical impedance of the robot's joints based on the performance and participation of the patient during the therapy session. The proposed strategy was evaluated in an active knee orthosis, designed and built by the researchers of the EESC/USP group in previous projects. A series elastic actuator drives the device and allows the implementation of joint impedance control.

**Keywords:** rehabilitation robotics, impedance control, adaptive control, exoskeleton

### INTRODUCTION

With a growing population of elderly people, the demand for physiotherapy services will rise for diagnoses associated with trauma-orthopedic lesions. Moreover, the number of recovering stroke patients has increased considerably worldwide. As a result, new rehabilitation procedures are being developed for additional home treatment, since the cost of a treatment in physiotherapy clinics is still high.

In recent years, the use of robots has generated significant advances in the medical field providing professionals new tools to treat patients. In an attempt to improve the confidence of patients with relation to a robotic rehabilitation system, an additional component very common nowadays is introduced: the computer games. This component provides a treatment focusing on the features of each individual, assisting the execution of tasks in specific contexts through visual feedback. Also, it integrates the cognitive component related to learning, which it is a necessary condition for rehabilitation of the movement (Hogan *et al.* (2006)).

Another crucial factor in the implementation of a robotic rehabilitation system is the contact between the patient and the robot, especially regarding the physical integrity of the user, already weakened by his/her condition. In this paper, we use impedance control (firstly developed in Hogan (1985)) to configure how the interaction takes place between patient and robot. The impedance control applied to the robot can operate at different times during the rehabilitation process, now promoting assistance to the motion, now resisting the movement of the patient. Such a robot are called interactive robots.

In this paper, we present the first results of an adaptive strategy that considers the control of the mechanical impedance of the robot's joints based on the performance and participation of the patient during the therapy session. The proposed strategy is divided in four subsystems, including estimation of absolute angular position of the robot's links, estimation of patient's active torques and stiffness based on EMG, and adaptation of the robotic stiffness according to patient participation.

The paper is organized as follows: Section presents an overview of the proposed adaptive variable impedance strategy, Section shows the results of the subsystem designed to the absolute values of the robot's links, Section presents the adaptive control solution based on EMG signals, and Section shows the final conclusions.

### ADAPTIVE VARIABLE IMPEDANCE STRATEGY

The proposed adaptive variable impedance strategy is divided in four subsystems as shown in Figure 1. The first subsystem aims to measure the actual position of the patient/robot system. The Robust Position Estimation subsystem uses the measures provided by joint encoders and inertial measurement units (IMUs) to obtain the absolute values of the links of the robot with relation to the ground and the joint angular positions. The proposed methodology is based on Markov Jump Linear Systems.

The Impedance Control subsystem should guarantee walking stability and ensure a smooth transition between the gait phases in the case of discrete variation of the impedance parameters ( $K_i^r$  and  $B_i^r$ ). The third subsystem consists



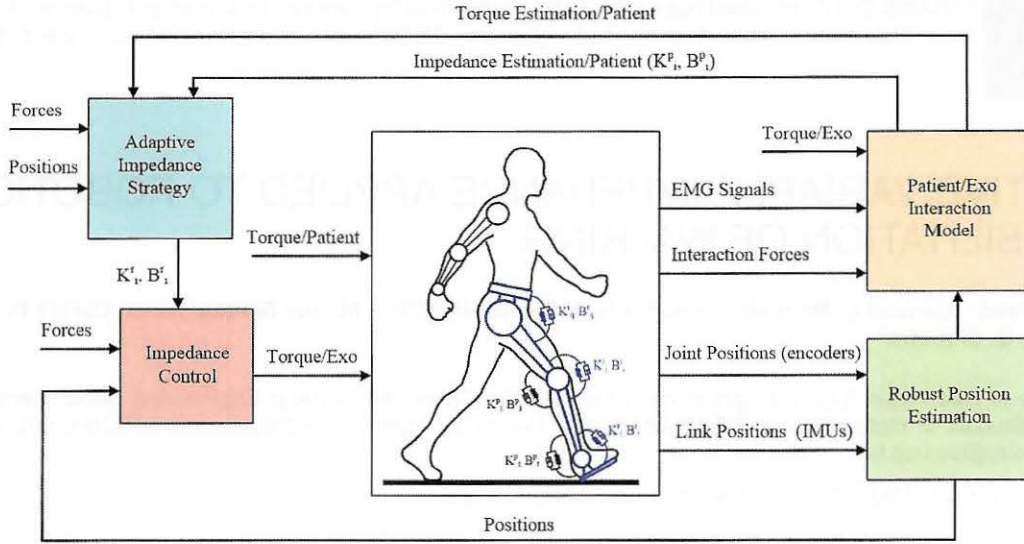


Figure 1 – adaptive variable impedance strategy.

in the identification of the actual conditions of the patient and the level of his/her participation during the robot-aided walking. The Patient/Exoskeleton Interaction Model considers EMG signals from the muscles and measures from the robot to estimate the torque provided by the patient and the patient's impedance parameters of each joint ( $K_i^p$  and  $B_i^p$ ). Finally, the fourth subsystem considers the data from the other subsystems to define the appropriate assistance of the robot according to the actual patient's participation, aiming to maximize his/her recovery. The Adaptive Impedance Strategy defines the robot's impedance parameters ( $K_i^r$  and  $B_i^r$ ) based on an optimization procedure, which properly represents the rehabilitation process and the interaction between patient and robot. A preliminary study of the proposed strategy was conducted considering the patient seated and performing alternated open-ended dorsi/plantarflexion movements with assistance of the Anklebot device. It is expected that the proposed adaptive strategy can result in a patient-tailored therapy, considering the specific and actual condition of the patient and defining the proper level of robot assistance.

## MARKOV JUMP LINEAR SYSTEMS-BASED POSITION ESTIMATION

In this section, the Markovian model and the sensor fusion strategy designed to estimate the absolute and relative angular positions of exoskeletons for lower limbs are presented.

### Gyroscope and Accelerometer Models

The IMUs are attached in each segment of the body as shown in Figure 2. Regarding the gyroscope measurement, the angular velocity of the link where the IMU is attached to,  $\dot{\theta}(t)$ , at a given instant  $t$ , is modeled as

$$\dot{\theta}(t) = \dot{\theta}_g(t) + b_g(t) + \eta_g(t), \quad \dot{b}_g(t) = -\frac{1}{\tau_g} b_g(t) + \eta_{b_g}(t), \quad (1)$$

where  $\dot{\theta}_g(t)$  is the angular velocity measured from the gyroscope in the Z axis,  $\eta_g(t)$  is a white Gaussian noise with variance  $\sigma_g^2$ ,  $b_g(t)$  is the gyroscope bias,  $\tau_g$  is the Markov process correlation time, and  $\eta_{b_g}(t)$  is a white Gaussian noise with variance  $\sigma_{b_g}^2$ .

Analogously, the acceleration of the link,  $a(t)$ , at a given instant  $t$ , is modeled as

$$a(t) = a_a(t) + b_a(t) + \mu_a(t), \quad \dot{b}_a(t) = -\frac{1}{\tau_a} b_a(t) + \mu_{b_a}(t), \quad (2)$$

where  $a_a(t)$  is the acceleration obtained from the accelerometer in the X axis of the local coordinate system,  $\mu_a(t)$  is a white Gaussian noise with variance  $\sigma_a^2$ ,  $b_a(t)$  is the accelerometer bias,  $\tau_a$  is the Markov process correlation time, and  $\mu_{b_a}(t)$  is a white Gaussian noise with variance  $\sigma_{b_a}^2$ .

### Sensor Fusion Strategy

Standard sensor fusions based on Kalman filters take into account the gyroscope signal as the main source for position estimation. They use the accelerometer signal as a redundant information to correct the estimated value from the gyroscope, usually corrupted by integration errors. The estimated angular velocity and bias from the gyroscope are given by

$$\hat{\dot{\theta}}_g(t) = \dot{\theta}_g(t) + \hat{b}_g(t), \quad \dot{\hat{b}}_g(t) = -\frac{1}{\tau_g} \hat{b}_g(t). \quad (3)$$

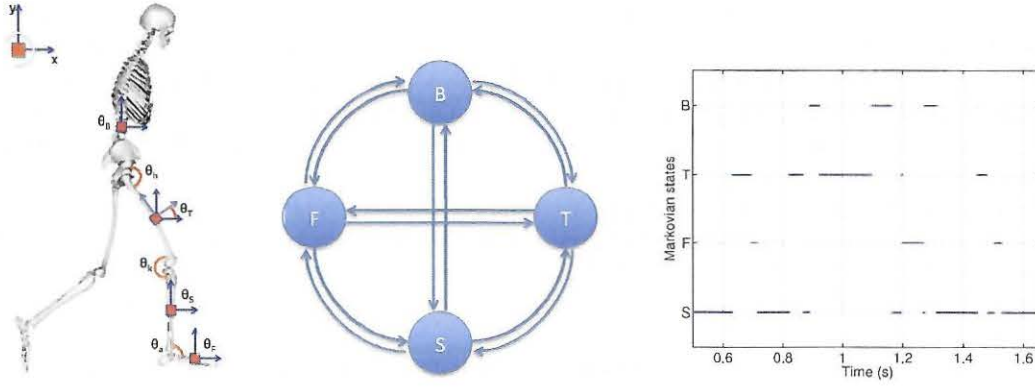


Figure 2 – IMUs attached to the body, MJLS estimation model, and Markovian state jumps over one step.

Taking the difference between real and estimated values gives

$$\Delta\dot{\theta}(t) = \dot{\theta}(t) - \dot{\hat{\theta}}_g(t) = \dot{b}_g(t) - \dot{\hat{b}}_g(t) + \eta_{b_g}(t) = \Delta b_g(t) + \eta_{b_g}(t), \quad (4)$$

and

$$\Delta\dot{b}_g(t) = \dot{b}_g(t) - \dot{\hat{b}}_g(t) = -\frac{1}{\tau_g}(b_g(t) - \hat{b}_g(t)) + \eta_{b_g}(t) = -\frac{1}{\tau_g}\Delta b_g(t) + \eta_{b_g}(t). \quad (5)$$

Hence, the state space representation of the estimation system is obtained as

$$\begin{aligned} \dot{x} &= Ax(t) + Bw(t), \\ \begin{bmatrix} \Delta\dot{\theta}(t) \\ \Delta\dot{b}_g(t) \end{bmatrix} &= \begin{bmatrix} 0 & 1 \\ 0 & -\frac{1}{\tau_g} \end{bmatrix} \begin{bmatrix} \Delta\theta(t) \\ \Delta b_g(t) \end{bmatrix} + \begin{bmatrix} 1 & 0 \\ 0 & 1 \end{bmatrix} \begin{bmatrix} \eta_{b_g}(t) \\ \eta_{b_b}(t) \end{bmatrix}, \end{aligned}$$

where  $\Delta\theta(t)$  and  $\Delta b_g(t)$  are respectively the position estimation and offset errors of the gyroscope.

The angular position obtained from the accelerometer is given by

$$\hat{\theta}_a(t) = \arcsin\left(\frac{a_a}{g_e}\right) = \theta(t) + \eta_a(t), \quad (6)$$

where  $g_e$  is the gravitational acceleration constant. Here, the measured acceleration,  $a_a$ , is assumed to contain only the component of the gravitational acceleration in the X axis. That is, no dynamic accelerations are presented.

The output equation of the state space representation is given by the difference between the estimated position from the accelerometer and estimated position from the gyroscope, that is,

$$z(t) = \hat{\theta}_a(t) - \hat{\theta}_g(t) = \theta(t) + \eta_a(t) - \hat{\theta}_g(t) = \Delta\theta(t) + \eta_a(t). \quad (7)$$

Therefore

$$z = Cx(t) + v(t) = \begin{bmatrix} 1 & 0 \end{bmatrix} \begin{bmatrix} \Delta\theta(t) \\ \Delta b_g(t) \end{bmatrix} + \eta_a(t). \quad (8)$$

The final estimated values for the angular position and gyroscope bias are given by

$$\hat{\theta}(t) = \hat{\theta}_g(t) + \hat{\Delta\theta}(t), \quad \hat{b}_g(t) = \hat{b}_g(t) + \hat{\Delta b_g}(t), \quad (9)$$

where  $\hat{\Delta\theta}$  and  $\hat{\Delta b_g}$  are the estimated values of the angular position and offset errors, respectively. These errors are estimated by the Kalman Filter using the sensor fusion approach.

## Markovian Estimation Model

In this section we propose a new MJLS model for angular position estimation of lower limbs exoskeletons. Considering one leg of an exoskeleton, see Figure 2, the following absolute and relative angles are defined:

- Absolute angles:  $\theta_B$  (body/trunk),  $\theta_T$  (thigh),  $\theta_S$  (shank),  $\theta_F$  (foot);
- Relative angles:  $\theta_h$  (hip),  $\theta_k$  (knee),  $\theta_a$  (ankle).

The spatial configuration of the exoskeleton Exo-Kanguera, at a given instant of time, can be obtained by estimating one absolute angle and three relative angles. The absolute angle is obtained by the sensor fusion approach presented in Section . The relative angles are measured by encoders coupled to the joint of the exoskeleton.

As show in Eq. (6), the estimated angular position from the accelerometer is obtained assuming absence of dynamic accelerations. Otherwise, the angle estimation given by the accelerometer deteriorates and this signal is not reliable.

In a regular human walking, all limb segments present substantial dynamic accelerations during some periods of time. We assume that the proposed MJLS-based model at a given instant of time, presents at least one reliable measurement of dynamic acceleration related with limb segments. We assume also that the measurements of the accelerometer attached to, can be used to estimate the angular position.

Figure 2 shows four Markovian states (B - Body, T - Thigh, S - Shank, and F - Foot) of the proposed MJLS model. They are defined as the condition where the related IMU presents small values of dynamic acceleration. In Figure 2 we show the time intervals where each IMU reaches the Markovian states condition for one step. The dynamic accelerations are estimated by computing the acceleration vector module, which includes all accelerometer axes, and comparing it to the gravitational acceleration.

The MJLS model for angular position estimation of lower limbs exoskeletons can be described by the following state-space equation

$$\dot{x}(t) = \bar{A}x(t) + \bar{B}w(t), \quad (10)$$

$$y(t) = \bar{C}(\Theta(t))x(t) + v(t), \quad (11)$$

where  $x(t) \in \mathbb{R}^n$  is the vector of states,  $w(t) \in \mathbb{R}^m$  and  $v(t) \in \mathbb{R}^q$  are respectively the vectors of the state and measurement noise,  $y(t) \in \mathbb{R}^q$  is the vector of output measurements, and  $\Theta(t)$  is the Markovian chain, with  $\Theta(t) = \{B, T, S, F\}$ . The vectors of states and output measurements are defined respectively as

$$x = [x_B \ x_T \ x_S \ x_F]^T \quad (12)$$

$$= [\Delta\theta_B \ \Delta b_B \ \Delta\theta_T \ \Delta b_T \ \Delta\theta_S \ \Delta b_S \ \Delta\theta_F \ \Delta b_F]^T,$$

$$y = [\Delta_{IMU} \ \Delta_h \ \Delta_k \ \Delta_a]^T \quad (13)$$

$$= [\hat{\theta}_{a_{IMU}} - \hat{\theta}_{g_{IMU}} \ \Delta\theta_B - \Delta\theta_T \ \Delta\theta_T - \Delta\theta_S \ \Delta\theta_S - \Delta\theta_F]^T,$$

where  $\Delta\theta_i = \theta_i - \hat{\theta}_{gi}$ , for  $i = \{B, T, S, F\}$  is the error between the value of the absolute angle of the segment  $i$  ( $\theta_i$ ) and the estimate of the angle calculated by the gyroscope ( $\hat{\theta}_{gi}$ );  $\Delta_{IMU}$  is the error between the estimate of the absolute angle calculated for a given segment by the accelerometer ( $\hat{\theta}_{a_{IMU}}$ ) and the estimate calculated by gyroscope ( $\hat{\theta}_{g_{IMU}}$ );  $\Delta_i$ , for  $i = \{h, k, a\}$ , is the estimation error of the relative angle of the joint  $i$ ; and  $\Delta b_i$ , for  $i = \{B, T, S, F\}$ , is the estimation error of the bias generated by the gyroscope in the segment  $i$ .

In the Markovian filter implementation, the segment associated with  $\Delta_{IMU}$  should present great measurement reliability from accelerometer data. Considering the gyroscope, accelerometer, and gyroscope bias models, matrices  $\bar{A}$  and  $\bar{C}$  are defined as

$$\bar{A} = \begin{bmatrix} 0 & 1 & 0 & 0 & 0 & 0 & 0 & 0 \\ 0 & -1/\tau_{g_B} & 0 & 0 & 0 & 0 & 0 & 0 \\ 0 & 0 & 0 & 1 & 0 & 0 & 0 & 0 \\ 0 & 0 & 0 & -1/\tau_{g_T} & 0 & 0 & 0 & 0 \\ 0 & 0 & 0 & 0 & 0 & 1 & 0 & 0 \\ 0 & 0 & 0 & 0 & 0 & -1/\tau_{g_S} & 0 & 0 \\ 0 & 0 & 0 & 0 & 0 & 0 & 0 & 1 \\ 0 & 0 & 0 & 0 & 0 & 0 & 0 & -1/\tau_{g_F} \end{bmatrix}, \quad \bar{C}(\Theta(t)) = \begin{bmatrix} M_B(t) & 0 & M_T(t) & 0 & M_S(t) & 0 & M_F(t) & 0 \\ 1 & 0 & -1 & 0 & 0 & 0 & 0 & 0 \\ 0 & 0 & 1 & 0 & -1 & 0 & 0 & 0 \\ 0 & 0 & 0 & 0 & 1 & 0 & -1 & 0 \end{bmatrix}, \quad (14)$$

where  $M_i$ , for  $i = \{B, T, S, F\}$ , assume values of 0 or 1 according to the angle associated to the value of  $\Delta_{IMU}$ . Thus, the only time-variant matrix is  $\bar{C}(t)$ .  $\bar{B}$  is an identity matrix.

In the proposed approach, only one inertial sensor is used at each instant in combination with three relative sensors. As the system has four inertial sensors, the Markovian model presents four states as shown in Figure Figure 2.

In Equation (14), four variables:  $M_B(t)$ ,  $M_T(t)$ ,  $M_S(t)$  and  $M_F(t)$  select the inertial sensor which will be used at each time instant. Table 1 presents the Markovian states and the related variable values.

After generating the estimation errors for all angles from the Markovian filter, the estimated absolute angles are given by  $\hat{\theta}_B = \hat{\theta}_{g_B} + \Delta\hat{\theta}_B$ ,  $\hat{\theta}_T = \hat{\theta}_{g_T} + \Delta\hat{\theta}_T$ ,  $\hat{\theta}_S = \hat{\theta}_{g_S} + \Delta\hat{\theta}_S$ , and  $\hat{\theta}_F = \hat{\theta}_{g_F} + \Delta\hat{\theta}_F$ .

## Results

This section presents simulated results obtained applying the standard position estimation and the proposed Markovian estimation approaches to an exoskeleton performing three steps. Figures 3, 4, 5 and 6 shows the results for all segments. As can be seen from Figure 3, the trunk segment features the most critical condition for angular estimation, since it has



large dynamic acceleration levels cumulatively from the other segments (thigh, shank and foot) in all stages of walking. Another problem is that the range of angular variations in this segment is too closed, and the static to dynamic acceleration ratio is too small, and the accelerometer has reliable signal only for few intervals. This behavior can be seen in Figure 3(a), where in standard case the intervals where correction occurs (update) using accelerometer are sparse, while in Figure 3(b) the Markov approach increased the reliability of using accelerometer data. Moreover, if we compare the average error and standard deviation of the estimated angle on the trunk, Figure 3(c), the MKF has lower mean error and smaller standard deviation compared to the KF. The same analysis can be extended to other segments of the exoskeleton.

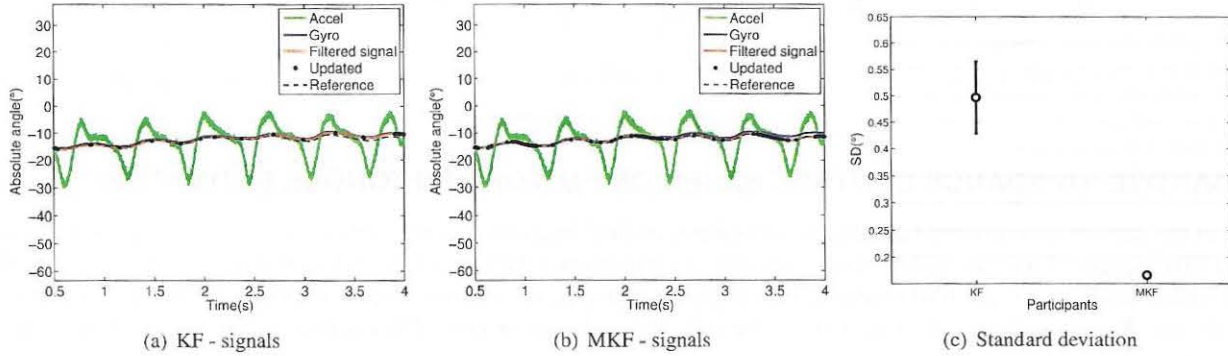


Figure 3 – Body/trunk segment.

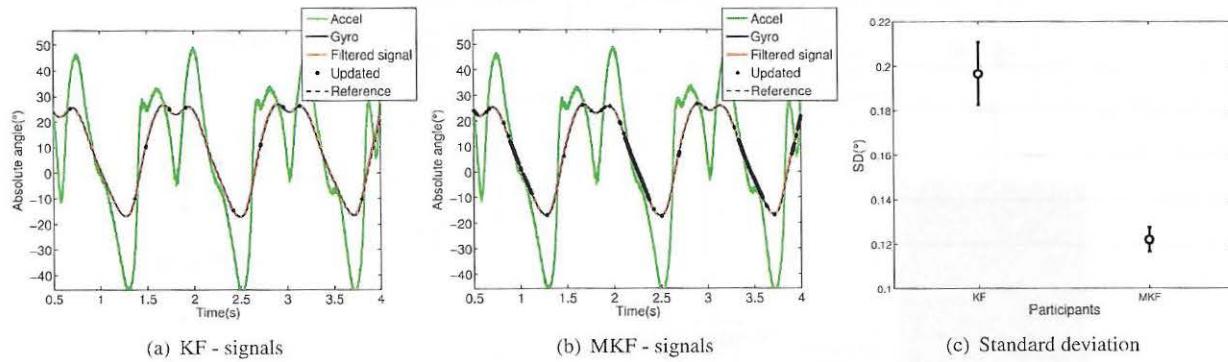


Figure 4 – Thigh segment.

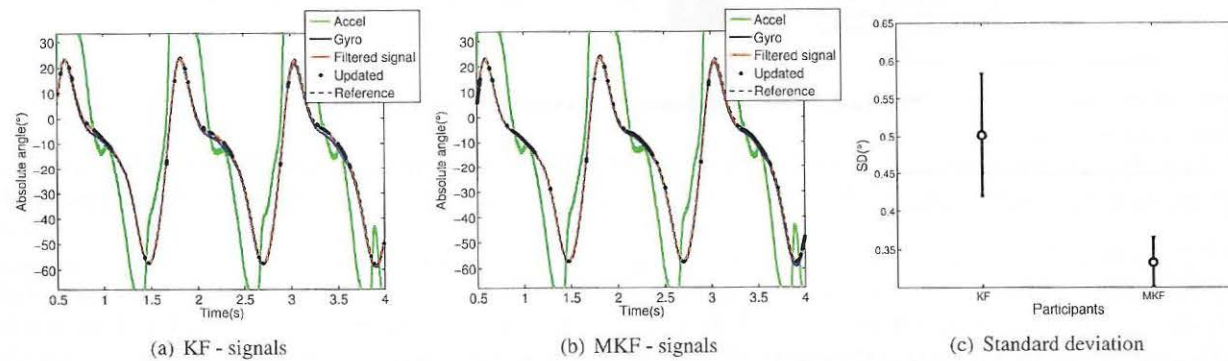


Figure 5 – Shank segment.

Table 1 – Table of Markovian States

Modes of Operation ( $\Theta(t)$ )	$M_B(t)$	$M_T(t)$	$M_S(t)$	$M_F(t)$
B	1	0	0	0
T	0	1	0	0
S	0	0	1	0
F	0	0	0	1

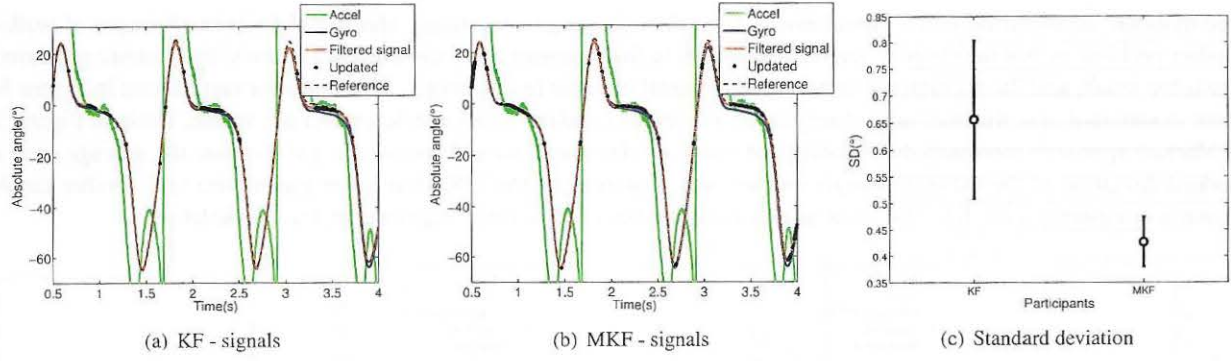


Figure 6 – Foot segment.

## ADAPTIVE IMPEDANCE CONTROL BASED ON EMG-DRIVEN TORQUE ESTIMATION

In this section, it is proposed an adaptive impedance control based on patient's torque estimation through measurement of EMG signals. First, an optimization procedure to adjust the EMG-driven model's parameters aiming to minimize the difference between the EMG-based estimate joint torque,  $\tau_{EMG}$ , and the torque estimated via Inverse Dynamics is proposed. Results obtained from an active knee orthosis is also presented. The optimization process is represented in Fig. 7.

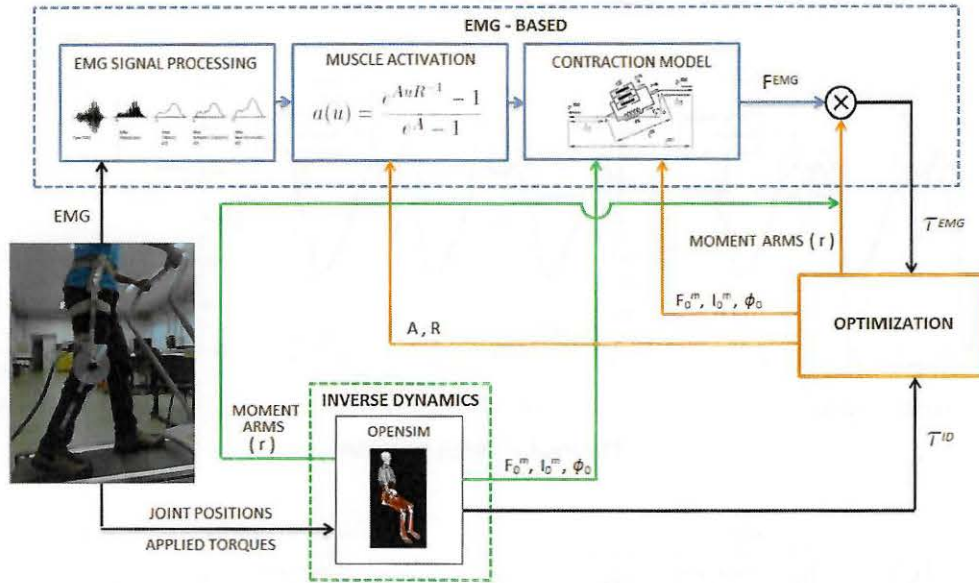


Figure 7 – Detailed diagram of optimization procedure.

The EMG signals pass through signal processing (with DC offset elimination, rectification, low-pass filtering, and subtraction of the measured offset when the muscle is relaxed); the processed signal is introduced into the muscle activation function. The result is used in the contraction model to generate muscle forces. Finally, the estimate torque is computed considering the the moments arms, obtained from the OpenSim model. On the other hand, joint positions and applied torques obtained from an active knee orthosis is loaded to the OpenSim model, and the Inverse Dynamics tool is used to compute  $\tau_{ID}$ . The active knee orthosis is also shown in Fig. 7. The orthosis' actuator is an rotary series elastic actuator, which allows to set the mechanical impedance of active knee orthosis (dos Santos (2015)). The experiment considers a healthy subject wearing the orthosis and performing movements of flexion and extension of knee, with the mechanical impedance of the actuator set to: 0 Nm/rad, 30 Nm/rad, and 60 Nm/rad. The user is sited with, initially, the knee in flexion at 90°.

After obtained the estimate torques, the optimization process adjust the parameters of the msucle models, see Jau-regui *et al.* (2015) for details. In Fig. 7, the green arrows are used to indicate that the parameters are taken from the Opensim software only at the beginning of the optimization process, which uses the *lsqcurvefit* algorithm of Optimization MATLAB®toolbox. EMG signals from five muscles involved in the movement of flexion/extension of knee are acquired: Rectus femoris, Vastus lateralis and Vastus medialis of the extensors group; and Biceps femoris e Semitendinosus, of flexors group.

Figure 8 shows the EMG-based estimate torque (blue) in comparison with the ID-based torque (red) of the three experiments with variable impedance. In this figure, it is observed that the EMG-based estimate torque has better approximation to the ID-based torque when the number of parameters increases; in the lower graph of this figure, it is also shown the estimated torque with parameters  $\alpha$  and  $A$  with larger limits.



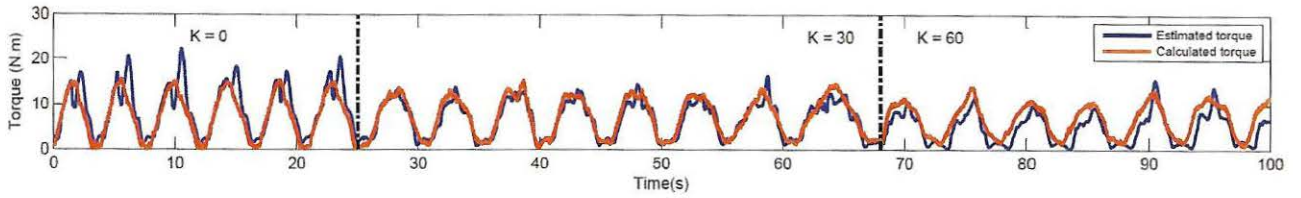


Figure 8 – Comparison of estimated and calculated torques for the three tests with variable impedance.

## Stiffness Estimation

The stiffness above the joint is given by the action of all acting muscles forces. When forces increase proportionally, no one movement is done, but the stiffness increase. A joint stiffness could be estimated considering a stiffness coefficient:

$$CR = \left| \sum_{i=1}^n F_i^{mt} r_i \right|_{Agonistas} + \left| \sum_{j=1}^m F_j^{mt} r_j \right|_{Antagonistas}, \quad (15)$$

Finally, the joint stiffness can be estimated as (Karavas et al., 2013):

$$K = \alpha CR + \beta, \quad (16)$$

where  $\alpha$  and  $\beta$  are constant parameters.

The same experiment shown in the last section is used to evaluate the stiffness estimation. First, the subject is asked to actively follow the desired trajectory (a metronome is used) for the three different degrees of robot's stiffness. Then, the subject is asked to relax the leg and let the robot does the whole work with stiffness set to 30 Nm/rad and 60 Nm/rad (with  $K_{exo} = 0$  Nm/rad and subject in passive condition there is no movement).

Figures 9 to 13 show the joint trajectories ( $\theta$ ) for twelve flexion and extension movements (here, total extension occurs at  $\theta = 90^\circ$ ), the subject's torque ( $\tau_{user}$ ) and stiffness ( $K_{user}$ ) estimates, the robot's torques ( $\tau_{exo}$ ), and the torque estimates for each muscle for the five conditions regarding robot's stiffness and subject participation (active or passive). Table 2 shows the RMS (root mean square) values for all signals. It is noteworthy that the subject's stiffness decreases with the increasing of the robot's stiffness, keeping the same amount of applied torque.

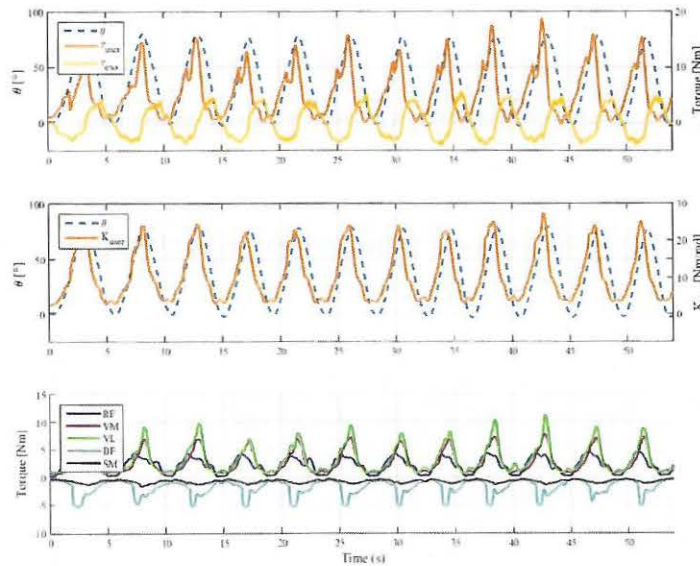


Figure 9 – Estimated stiffness and torques. Active subject and  $K_{exo} = 0$  Nm/rad.

Table 2 – RMS values.

Robot's stiffness $K_{exo}$ [Nm/rad]	Subject's stiffness $K_{user}$ [Nm/rad]		Subject's torque $\tau_{user}$ [Nm]		Robot's torque $\tau_{exo}$ [Nm]	
	Active	Passive	Active	Passive	Active	Passive
0	12.57	-	6.76	-	2.69	-
30	9.98	3.50	5.31	0.73	1.62	4.45
60	7.77	4.08	6.41	2.97	2.05	4.39

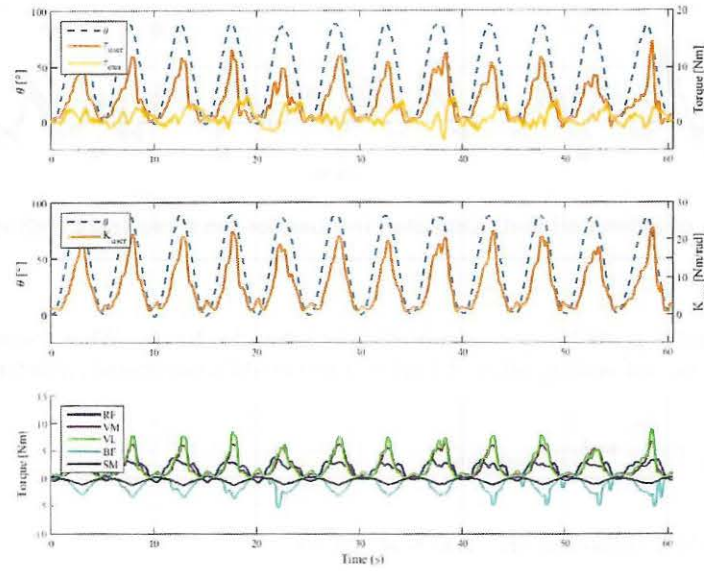


Figure 10 – Estimated stiffness and torques. Active subject and  $K_{exo} = 30$  Nm/rad.

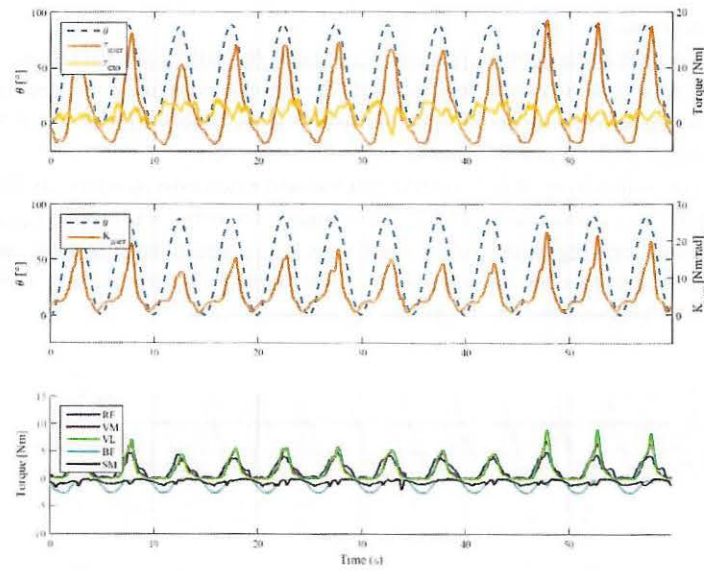


Figure 11 – Estimated stiffness and torques. Active subject and  $K_{exo} = 60$  Nm/rad.

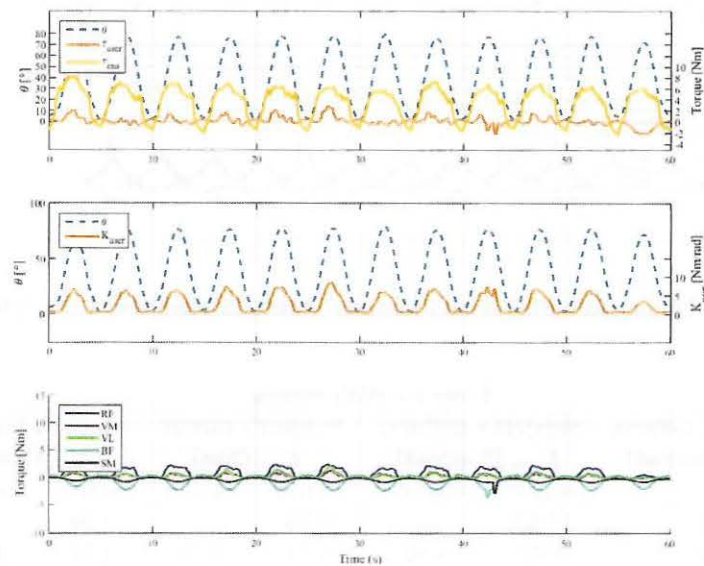


Figure 12 – Estimated stiffness and torques. Passive subject and  $K_{exo} = 30$  Nm/rad.



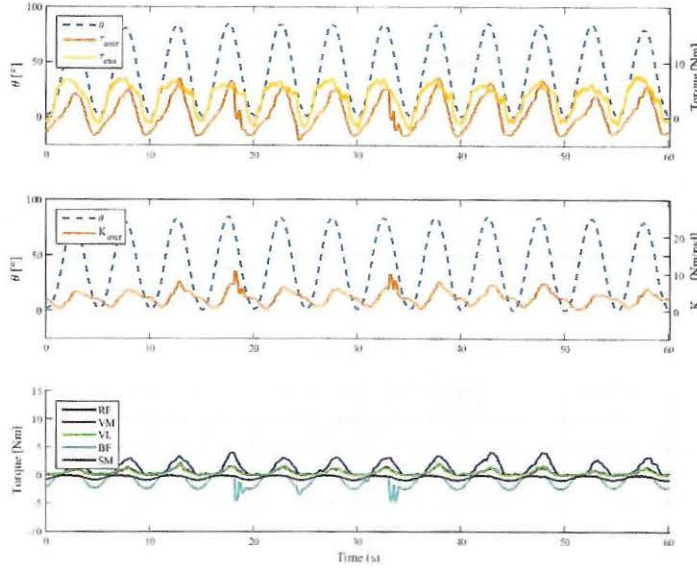


Figure 13 – Estimated stiffness and torques. Passive subject and  $K_{exo} = 60$  Nm/rad.

### Adaptive Control Strategy

In this section, the proposed adaptive strategy to defined the robot's stiffness is presented. First, it is assumed that exoskeleton and user are trying to perform the same task. In this case, the dynamical equation that defines the system is given by:

$$\tau_{user} + \tau_{exo} = M(\theta)\ddot{\theta} + C(\theta, \dot{\theta}) + G(\theta), \quad (17)$$

where  $M(\theta)$  is the inertial matrix,  $C(\theta, \dot{\theta})$  is the vector of Coriolis and centripetal forces and  $G(\theta)$  the vector of gravitational forces corresponding to the coupled dynamic system. We also assume that the cooperation task between exoskeleton and the user needs a known torque to be executed, as presented in Perez-Ibarra *et al.* (2014). This torque will be the sum of the torque contributions of each participant in the task, that is,  $\tau_{nec} = \tau_{user} + \tau_{exo}$ . We assume the robot is controlled by an impedance control law given by:

$$\tau_{exo} = K_{exo}\theta_e - B_{exo}\dot{\theta} \quad (18)$$

where  $\theta_e$  is position error given by the difference between desired and measured position,  $\dot{\theta}$  the angular velocity,  $K_{exo}$  and  $B_{exo}$  are the stiffness and damping defined by the designer. Following the same structure, we assume the user perform a similar impedance control strategy with:

$$\tau_{user} = K_{user}\theta_e - B_{user}\dot{\theta}, \quad (19)$$

where  $K_{user}$  and  $B_{user}$  are the user's stiffness and damping, respectively.

Using 18 and 19, and considering steady state conditions (where the term of damping, directly affected by velocity, will be null):  $\tau_{nec} = (K_{exo} + K_{user})\theta_e$ . Consequently, robot stiffness could be calculated as:

$$K_{exo} = \frac{\tau_{nec}}{\theta_e} - K_{user} = K_{nec} - K_{user}, \quad (20)$$

since stiffness is by definition the ratio between force and position. From eq.(15) it is possible to observe that when user does not participate of the task, i.e.  $K_{user} = 0$ , the robot assume the highest stiffness to assist the whole movement. To avoid abrupt changes in robot stiffness, it is included an adaptation factor  $0 < f < 1$ , to limit the effective stiffness of the exoskeleton, then, for a given time instant  $i$ :

$$K_{exo}(i) = fK_{exo}(i-1) + (1-f)[K_{nec} - K_{user}(i)]. \quad (21)$$

Thus, for small values of  $f$ , variation among previous and actual stiffness is considerable.

To evaluate the proposed adaptive strategy for robot's stiffness, in the second experiment the subject is asked to keep the knee flexed at  $\theta = 90^\circ$  (different from previous figures, total extension occurs at  $\theta = 0^\circ$ ) while in stand posture. For simplicity, EMGs signals of only one flexor muscle (biceps femoris) and one extensor muscle (rectus femoris) are measured to sense activity during knee flexion and extension movements. The set point for the active knee orthosis is set to  $\theta = 90^\circ$ . The necessary stiffness ( $K_{nec}$ ) is defined as the minimum stiffness to take the subject's leg (without collaboration of him) from  $0^\circ$  to 10% of the set point ( $81^\circ$ ). For this experiment,  $K_{nec}$  is set as 30 Nm/rad.

Figure 14 shows the set point position ( $\theta_d$ ), the measured position ( $\theta$ ), the necessary stiffness to maintain the set point position ( $K_{nec}$ ) and the user's stiffness ( $K_{user}$ ) estimated by 16, and the exoskeleton's stiffness ( $K_{exo}$ ) calculated by 21. Note that the when the subject increases the stiffness, the exoskeleton and user system reaches the set point with a decreasing of the robot's stiffness as expected.

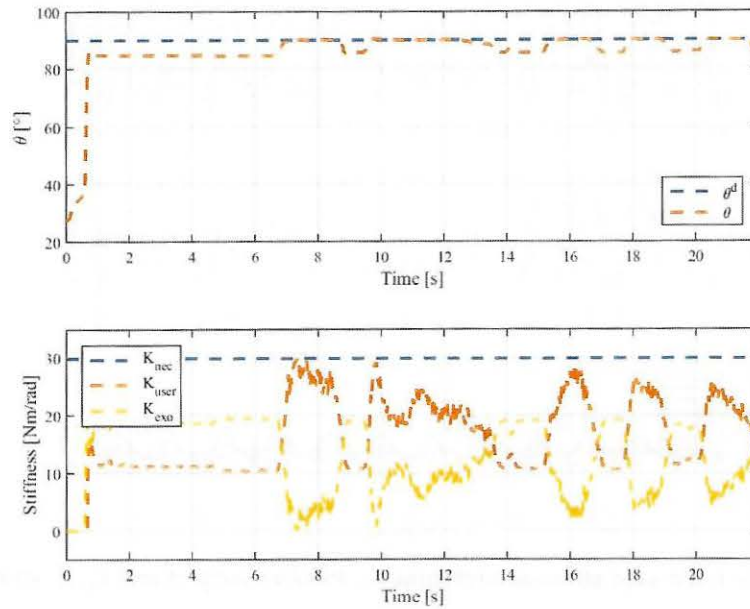


Figure 14 – Stiffness behavior to maintain the set point position during right leg flexion.

## CONCLUSIONS

This paper describes our ongoing efforts to develop adaptive impedance strategies for robot-aided walking rehabilitation of post-stroke patients. First, a robust position estimation system is proposed to measure the absolute angular position of the robot's links. In the sequence, an adaptive control solution based on EMG signals is proposed. The preliminary results show the proposed adaptive strategy based on patient's torque and stiffness estimation is suitable for adjustment of robot impedance. Future works include the proposal of new adaptive control laws for the robot's control parameters in order to improve the patient's participation during the robotic therapy session.

## ACKNOWLEDGMENTS

This work was supported by FAPESP under grant no. 2013/14756-0.

## REFERENCES

- dos Santos, W. M., Caurin, G. A. P., Siqueira, A. A. G., 2015, Design and control of an active knee orthosis driven by a rotary Series Elastic Actuator, "Control Engineering and Practice", pp. 1-12.
- Hogan, N., Krebs, H. I., Rohrer, B., Palazzolo, J. J., Dipietro, L., Fasoli, S. E., Stein, J., Frontera, W. R. and Volpe, B. T., 2006, Motions or Muscles? Some Behavioral Factors Underlying Robotic Assistance of Motor Recovery, "Journal of Rehabilitation Research and Development", Vol. 43, No. 5, pp. 605-618.
- Hogan, N., 1985, Impedance control: An approach to manipulation, Parts 1-3., "Journal of Dynamic Systems, Measurement, and Control", pp. 1-24.
- Jauregui, B. S., Peña, G. G., Siqueira, A. A. G., 2015, "An Optimized EMG-Driven Model for Patient Torque Estimation Applied to Rehabilitation Robotics", Proceedings of the 23rd Brazilian Congress of Mechanical Engineering, Vol.1, Rio de Janeiro, Brazil, pp. 1-6.
- Perez-Ibarra, J. C. P., dos Santos, W. M., Krebs, H. I. and Siqueira, A. A. G., 2014, "Adaptive impedance control for robot-aided rehabilitation of ankle movement", Proceedings of the 5th IEEE RAS EMBS International Conference on Biomedical Robotics and Biomechatronics, pp. 664-669.

## RESPONSIBILITY NOTICE

The authors are the only responsible for the material included in this paper.